Paper No.
06576

CORROSION NACExpo 2006
61ST ANNUAL CONFERENCE & EXPOSITION

PREDICTION AND ASSESSMENT OF AMMONIUM BISULFIDE CORROSION UNDER REFINERY SOUR WATER SERVICE CONDITIONS

Richard J. Horvath
Shell Global Solutions (US) Inc.
P.O. Box 4327
Houston, TX 77210

Michael S. Cayard [(1)]
Flint Hills Resources, LP
P.O. Box 64596
St. Paul, MN 55164

Russell D. Kane
Honeywell Process Solutions [(2)]
14503 Bammel N. Houston Road, Suite 300
Houston, TX 77014

ABSTRACT

This paper summarizes results of a joint industry program (JIP) to address ammonium bisulfide (NH_4HS) corrosion in H_2S-dominated alkaline sour waters typically found in refinery services such as the reactor effluent air cooler (REAC) systems of hydroprocessing units. The impacts of several process variables on corrosion were quantified. Key learnings support a paradigm shift from the rules of thumb previously applied to these systems. Data collected were used to develop a software tool to predict the corrosion rate of 14 materials evaluated in the program.

Keywords: sour water, ammonium bisulfide, NH_4HS, hydrogen sulfide, H_2S, partial pressure, isocorrosion diagram, temperature, chloride, hydrocarbon, velocity, wall shear stress, ammonium polysulfide, APS, imidazoline, materials selection, software, reactor effluent air cooler, REAC, hydroprocessing, refining.

---

(1) Formerly with InterCorr International, Inc.
(2) Acquired InterCorr International, Inc.

INTRODUCTION

The subject of alkaline sour water corrosion in petroleum refineries over the past 25 years has been addressed in the literature.[1] However, despite the prevalence of sour water corrosion problems in refining operations, there has been very little ammonium bisulfide corrosion data published in the open literature. Additionally, most of these studies had not specifically investigated the impact of velocity or a wide range of exposure conditions. The approach used in many studies had been to focus on empirical findings heavily relying on evaluations of operational experience. Hence, there was a need for more precise and quantitative data on ammonium bisulfide corrosion for a variety of materials under simulated service conditions. These data were needed as a technical basis for improved prediction of ammonium bisulfide corrosion for use in materials selection, control of process unit operation to mitigate corrosion, and assessment of chemical treatments.

Previous Investigations

Perhaps the most notable paper by R. L. Piehl[2] describes a survey conducted by NACE Group Committee T-8 (now Specific Technology Group [STG] 34) covering corrosion in the reactor effluent air coolers and associated piping in 42 hydrocrackers and hydrotreaters. Analysis of the survey results established that sour water corrosion was mild to negligible when the NH_4HS concentration was 2 wt% or less and the velocity was 20 ft/s (6.1 m/s) or less. This experience has been generally utilized by the industry for control of sour water corrosion in hydroprocessing unit reactor effluent air coolers, and has served the industry well when followed. Although an actual corrosion threshold was not identified by the survey results, it was noted that corrosion rates may be severe above 3 – 4 wt% NH_4HS concentration.

Damin and McCoy[3] reported results of laboratory corrosion tests conducted in a stirred autoclave over the NH_4HS concentration range of 10 – 45 wt%. They measured low corrosion rates for carbon steel and type 316 stainless steel (UNS S31600) up to about 35 wt% NH_4HS concentration. Above that, the corrosion rate of both materials increased rapidly to extremely high rates of attack. Their test results appeared to demonstrate the presence of a threshold NH_4HS concentration at which the corrosion resistance of the materials changed dramatically. They postulated that this was the result of the formation of a metal-ammonium complex that could act to strip the normally protective iron sulfide film from the metal surface. It should be noted that the 35 wt% NH_4HS concentration threshold was observed at near-stagnant conditions in a stirred autoclave.

The only laboratory corrosion data documenting the effect of velocity on NH_4HS corrosion was reported by Scherrer et al.[4] In their tests, conducted with 4.5 − 10 wt% NH_4HS, the corrosion rate of carbon steel increased by 40 − 64% when increasing the velocity from 11 ft/s (3.4 m/s) to 21 ft/s (6.4 m/s), the highest velocity tested.

Predictive Capabilities

It was readily evident from the published studies cited above that there were insufficient corrosion data to fully understand and predict the corrosiveness of ammonium bisulfide solutions over a wide range of concentration and velocity. A recent American Petroleum Institute (API) survey on corrosion in refinery sour water systems also indicated similar findings.[5] The effect of other parameters such as pH, temperature, partial pressures of H_2S and NH_3, and solution contaminants such as oxygen, chlorides, and cyanides were not quantified. Additionally, compared to carbon steel, there were even

less corrosion data available for many alloys commonly used in this service. For example, no data were found for alloy 2205 (UNS S31803), which in recent years has been used in the higher NH_4HS concentration systems. Experience surveys have been conducted, but have restricted applicability due to limited availability of information. However, these studies have identified the extent of corrosion problems in process units handling alkaline sour water and the critical needs related to these units in terms of improving predictive capabilities and system reliability.

Some operating companies and process licensers have developed their own procedures for controlling NH_4HS corrosion of carbon steel based on operating experience. In many instances, these permit concentrations of NH_4HS exceeding the 2 wt% concentration recommended by Piehl, perhaps up to the 8 − 10 wt% range, while maintaining the 20 ft/s (6.1 m/s) maximum velocity criteria. Furthermore, there are some hydroprocessing units with carbon steel reactor effluent systems that have actually operated for periods of time with NH_4HS concentration in the 15 − 20 wt% range.

It has not been uncommon for hydroprocessing units, designed to handle a given NH_4HS concentration, to be exposed to higher concentrations when the nitrogen level in the feed is increased without a corresponding increase in the injection rate of wash water. This usually results in increased corrosion and in some cases unit reliability problems and unscheduled shutdowns. Within the last 25 years, there have been several major incidents where NH_4HS corrosion caused loss of containment in hydroprocessing units that resulted in damage/lost production on the order of $50 million US.

PROGRAM OVERVIEW

InterCorr International, Inc., in collaboration with Shell Global Solutions (US) Inc., initiated a JIP entitled "Prediction and Assessment of Ammonium Bisulfide Corrosion Under Refinery Sour Water Service Conditions."[6] Phase I of this program, commonly referred to as the Sour Water JIP, was conducted from March 2000 to February 2003. The final program report was issued in June 2003 to the 16 refining and engineering companies that jointly sponsored this program.[7]

The goal of this program was to develop a quantitative engineering database and guidelines to predict corrosion in H_2S-dominated alkaline sour water systems as a function of NH_4HS concentration, velocity (wall shear stress), H_2S partial pressure, temperature, chloride concentration, hydrocarbon content and chemical treatments.

Program Tasks

The program included five tasks. The first four tasks involved data development using a specialized laboratory flow loop designed specifically to handle the environments and particulars associated with conducting experiments in NH_4HS solutions. The final task involved the development of a comprehensive software tool to predict corrosion rates of the materials tested in the NH_4HS environments.

First Task. The first task of the program involved developing comprehensive baseline isocorrosion curves to enable determination of corrosion rates for 14 materials ranging from carbon steel to alloy C-276 (UNS N10276) as a function of NH_4HS concentration and flow loop velocity. This work focused on the development of NH_4HS corrosion rate data in H_2S-dominated systems with H_2S partial pressure (P_{H2S}) of 50 psia (340 kPa absolute) and a temperature of 130°F (55°C). Data were obtained at NH_4HS concentrations ranging from 1 wt% to 30 wt% and velocities in the flow loop

ranging from 0 to 80 ft/s (24 m/s). This first task was designed based on relatively simple matrices. This allowed for maximum experimental control to clearly establish trends in corrosion rate as an independent function of NH_4HS concentration and flow loop velocity. These data were obtained by the major oil company prior to the initiation of the JIP and were licensed to the JIP sponsors as part of the JIP participation agreements. These baseline data were used for comparison to the subsequent JIP-developed data that focused mainly on parametric effects.

A first subtask involved experiments designed to investigate the parametric effect of H_2S partial pressure on the corrosion rate in NH_4HS environments. Additional tests were conducted at P_{H2S} = 30 psia (210 kPa absolute), 100 psia (690 kPa absolute) and 150 psia (1,000 kPa absolute) for comparison with the baseline data at P_{H2S} = 50 psia (340 kPa absolute).

Second Task. The second task involved experiments designed to investigate the parametric effects of two key process variables – temperature and chloride concentration. In addition to the baseline temperature of 130°F (55°C), a series of tests were conducted at 190°F (88°C) and 250°F (121°C). In addition to the baseline chloride concentration of zero, a series of tests were conducted at 100 ppm and 1,000 ppm chloride. The chloride ion concentration was attained by the addition of HCl.

Third Task. The third task involved experiments designed to investigate the effect of hydrocarbon/sour water mixtures on NH_4HS corrosion. Refinery liquid hydrocarbon systems sometimes become contaminated with small quantities of sour water due to carryover. Additionally, sour water environments can contain small amounts of hydrocarbons. In some areas of hydroprocessing units, multiphase environments (oil/gas/water) are present. This task examined the role of hydrocarbons in effectively inhibiting NH_4HS corrosion. The test matrix incorporated both light and heavy hydrocarbons. Experiments covered hydrocarbon contents in the range of 10 to 98 vol%, with data for 0 vol% hydrocarbon (100 vol% sour water) available from the first task. All testing was conducted at 130°F (55°C) and two H_2S partial pressures, 50 psia (340 kPa) and 100 psia (690 kPa). The effect of wall shear stress on the corrosion performance was also examined with the heavy hydrocarbon.

Fourth Task. The fourth task evaluated the performance of two chemical treatments on NH_4HS corrosion, namely ammonium polysulfide (APS) and imidazoline. Testing was conducted in selected environments to spot check their ability to reduce the corrosion rates, as well as compare the performance between the two chemical treatments evaluated. NH_4HS concentrations ranged from 2 to 20 wt% with the majority of the testing at 8 wt%. The testing was primarily conducted at 130°F (55°C), with a few tests conducted at 190°F (88°C) to evaluate the impact of temperature. Chemical treatments were conducted based on ppmv neat chemical and the dosages ranged from 50 to 500 ppmv.

Fifth Task. The fifth task involved the development of a user-friendly software tool to predict NH_4HS corrosion rates. This software tool would combine the data obtained in this JIP with flow modeling calculations on plant tube/piping configurations to predict the NH_4HS corrosion rates of the 14 materials tested.

Materials Evaluated

Fourteen (14) materials were evaluated in this program, ranging from carbon steel to alloy C-276. A list of the materials evaluated and their nominal compositions is provided in Table 1. These materials were procured in round bars for machining of the flow-through coupons and in plate or sheet for preparation of the flat corrosion coupons evaluated in the static zone of the flow loop.

EXPERIMENTAL PROCEDURES

Several aspects of the experimental procedures are described including a general description of the test facility, description of the flow-through and static corrosion coupons and ionic modeling conducted to determine the quantity of chemical ingredients to simulate the intended test conditions.

Test Facility

A clever test technique was required for this program due to the sensitivity of sour water environments to contamination by oxygen, and the high velocities required to obtain meaningful results that could be applied to the field. The test methodology, originally conceived by the major oil company, incorporated an internal gear pump driven by a magnetically coupled spinning attachment. The design allowed for continuous flow velocities up to 80 ft/s (24 m/s) through the flow-through corrosion coupons and continuous control of test temperature. Because the test fluid was constantly recirculated within a pressurized test autoclave, the risk of oxygen contamination was minimized. Another advantage of this test facility was the rigorous simulation of wall shear stresses in liquid-full flow through the flow-through corrosion coupons that could be correlated with a wide range of flow regimes in service.

Corrosion Coupons

Two types of mass-loss corrosion coupons were utilized. The flow-through coupons subjected to the fluid passing through the pump consisted of ½-inch (12.7-mm) OD by ¾-inch (19-mm) long coupons with a 0.15-inch (3.8-mm) ID bore that was exposed to the sour water test solution. Six flow-through coupons were evaluated in each test. Each coupon was electrically isolated from the others and from the coupon holder assembly using polytetrafluoroethylene (PTFE) or polyetheretherketone (PEEK) washers that also contained a 0.15-inch (3.8-mm) ID bore. The OD of the flow-through coupons was shielded from the sour water test solution with heat shrink tubing and further contained in an alloy C-276 tubular coupon holder.

Corrosion coupons were also mounted in two stacks of three coupons underneath the pump to provide static mass-loss corrosion rate results. These static zone corrosion coupons were also useful to verify the corrosion rate trends observed on the flow-through coupons. The static zone coupons were standard 2.0-inch (51-mm) long by 0.500-inch (12.7-mm) wide by 0.125-inch (3.18-mm) thick flat coupons with two ¼-inch (6.35-mm) diameter holes for mounting.

Test Protocol

Solution preparation and subsequent saturation with H_2S were conducted external to the test autoclave in a glass mixing vessel. Based on the ionic modeling, discussed below, the prescribed amount of distilled water was placed in the glass mixing vessel and purged with nitrogen. Reagent grade ammonium hydroxide (NH_4OH) was then added to the mixing vessel in the prescribed quantity. A very small volume of dilute sodium cyanide (NaCN) solution was injected into the mixing vessel to react with any remaining trace of oxygen. The solution was then completely saturated with ultrapure H_2S gas (< 1 ppm oxygen) prior to transfer to the test autoclave.

Earlier in the testing protocol, the flow-through corrosion coupons and flat corrosion coupons for the static zone were cleaned, measured, and pre-weighed. The stack of six flow-through coupons was assembled and all coupons were stored in a desiccator until being mounted onto the pump prior to the testing. The required pump speed to attain the desired test velocity was determined by calibration with water. After the water calibration, the pump, autoclave head and associated fixturing were thoroughly dried. The test coupons (flow-though stack and static coupons) were then mounted onto the pump and the autoclave head with pump assembly was assembled onto the autoclave body. The autoclave was pressure tested with nitrogen and then evacuated under vacuum and backfilled with nitrogen five times to deaerate the autoclave and pump assembly.

The nitrogen was then evacuated under vacuum and the autoclave was backfilled with H_2S. A slight H_2S pressure was placed on the glass mixing vessel containing the H_2S-saturated NH_4HS solution to transfer the solution to the autoclave. Additional H_2S was added to the autoclave to achieve the desired H_2S partial pressure. Pump flow was initiated and the speed adjusted to attain the desired test velocity as the autoclave was heated to test temperature. Solution pH was monitored at test initiation, midway through the test, and at test conclusion.

In the tests that contained hydrocarbon/sour water mixtures and chemical treatments, an impeller positioned in the bottom of the autoclave was used to mix the solution in the autoclave during the test. This was particularly important at high hydrocarbon fractions and/or low test velocities to maximize the mixing of the multiphase test solution.

Each flow loop experiment was conducted for 48 hours at test conditions. After the final pH measurement, the pump and heat were switched off, the autoclave head pressure was bled down through a vent scrubber containing caustic, and the test solution was pushed out into a caustic scrubber under nitrogen pressure. Caustic solution was pushed into the test autoclave and circulated through the pump at a low speed. The caustic was pushed out and water was pushed into the autoclave to rinse. Once the water was removed, the autoclave was opened and the corrosion coupons were retrieved for cleaning and corrosion rate determination. A water calibration check was performed to verify the flow rate versus pump speed. The autoclave and pump assembly were then cleaned thoroughly prior to running the next test.

Ionic Modeling

Ionic modeling studies were conducted to determine the appropriate amounts of distilled water and NH_4OH required to achieve the desired NH_4HS concentration in equilibrium with the desired H_2S partial pressure and total vapor pressure at test temperature. The ionic modeling studies were conducted by the major oil company staff, using the ASPEN OLI[3] flowsheeter version 11, and MS Excel[4] spreadsheet. The ionic model contains a special "electrolytes package" and allows calculation of the phase behavior of an aqueous NH_4HS solution in equilibrium with its vapor as a function of temperature, pressure and composition. It was critical to the design of suitable experiments to model actual process unit conditions, within the constraints of available laboratory equipment. To model a test at prescribed temperature, NH_4HS concentration and H_2S partial pressure, it calculates the amount of distilled water, concentrated NH_4OH and the total pressure required. The model further determines the "closed cup" pH at both ambient temperature and the test temperature. In the experiments containing

[3] ASPEN OLI is a joint product of Aspen Technology Inc.'s ASPEN PLUS flowsheeter and the OLI Engine product of OLI Systems Inc. Both pieces are independently licensed from each vendor and assembled by the client.
[4] MS Excel is a spreadsheet product of Microsoft Corporation.

hydrocarbons, the ionic modeling became significantly more complex, but was successfully used to design the experiments.

The ionic modeling was used to study the influence of NH_4HS concentration and H_2S partial pressure on pH. The results are shown in Figure 1. As expected, the pH increases with an increase in NH_4HS concentration and a decrease in H_2S partial pressure.

During the first task, the pH values predicted by the ionic modeling were compared to measured values of pH over the range of 1 to 30 wt% NH_4HS at an H_2S partial pressure of 50 psia (340 kPa absolute). The measured pH values were in excellent agreement with the ionic model predictions, as shown in Table 2.

RESULTS AND DISCUSSION

Baseline Isocorrosion Diagrams

The data development conducted under the first task was the most significant to the overall program, as it established the baseline corrosion rates to which data from the remaining tasks were compared. The baseline data were collected at 50 psia (340 kPa absolute) H_2S partial pressure and at a temperature of 130°F (55°C). The test matrix involved NH_4HS concentrations that varied from 1 to 30 wt% and test velocities that varied from 10 to 80 ft/s (3.0 to 24 m/s). Corrosion rates measured on the static corrosion coupons at the lowest test velocity were used to represent the corrosion rates at 0 ft/s (0 m/s) for each material.

A total of 32 independent tests were conducted and included six materials in each test. Obviously with the inclusion of 14 materials in this test program, decisions regarding which materials to include in a particular test were required. Selection of the materials was based on the performance of the materials in other tests. For instance, once the material exhibited high corrosion rates at a particular NH_4HS concentration and/or velocity, it was replaced with a more resistant material in tests conducted at more severe conditions. All other test conditions were the same for all tests. The corrosion rate results for each material were plotted on a graph at the respective test conditions, with NH_4HS concentration on the X axis and the flow velocity on the Y axis. Isocorrosion lines were drawn at appropriate corrosion rate values to produce isocorrosion diagrams for each of the 14 materials tested.

The resulting isocorrosion diagram for carbon steel is provided in Figure 2. The location and shape of the isocorrosion curves indicate there are three discrete corrosion regimes at the baseline test conditions — P_{H2S} = 50 psia (340 kPa absolute) and 130°F (55°C).

1. At low NH_4HS concentrations (2 wt% or less), low corrosion rates are observed at low velocity. In this regime, corrosion rates increase only marginally with increased test velocity. The maximum corrosion rate measured at 2 wt % NH4HS was 28 mpy (0.7 mm/y) at 80 ft/s (24 m/s).
2. At intermediate NH_4HS concentrations (2 – 8 wt%), low to moderate corrosion rates are observed. However, these corrosion rates increase markedly with an increase in test velocity. The maximum corrosion rate measured at 8 wt% NH_4HS was 166 mpy (4.2 mm/y) at 80 ft/s (24 m/s).
3. At high NH_4HS concentrations (greater than 8 wt%), moderate to high corrosion rates are observed at low velocity. As with the intermediate NH_4HS concentrations, the corrosion rates

also increase markedly with an increase in test velocity. The maximum corrosion rate measured at 30 wt % NH_4HS exceeded 800 mpy (20 mm/y) at 80 ft/s (24 m/s).

The isocorrosion diagrams for the alloy materials tested, such as alloy 825 (UNS N08825), indicated that the isocorrosion curves were shifted upwards and towards the right, as compared to the isocorrosion curves of the same corrosion rate values for carbon steel, indicating the increase in material resistance. Alloy 825 demonstrated excellent corrosion resistance at the baseline conditions up to 8 wt% NH_4HS, which agrees well with industry experience to date. However, alloy 825 was not fully resistant to NH_4HS corrosion, as many have believed. Although alloy 825 retained its corrosion resistance at very low velocity, its corrosion rate increased steadily with increasing NH_4HS concentration at higher velocities, and exceeded 10 mpy (0.25 mm/y) at some test conditions.

Several observations were made regarding the performance of the alloys. Alloy 400 (UNS N04400) was not much better than carbon steel over the range of NH_4HS and velocities investigated. Type 304 stainless steel (UNS S30400) exhibited performance similar to type 316 stainless steel. Despite the current industry belief that alloy 2205 was suitable to mitigate corrosion in REAC systems, it was found to corrode at intermediate and high NH_4HS concentrations, especially at high velocities. Alloy 625 (UNS N06625) was significantly better than alloy 825 at intermediate and high NH_4HS concentrations. Alloy C-276 was found to be resistant to NH_4HS at all conditions evaluated in this task.

When using these data, it is important to note that the velocity plotted on the isocorrosion diagrams corresponds to the velocity of sour water through the 0.15-inch (3.8-mm) ID bore of the flow-through coupons. Corrosion rate measured at any test velocity does not equate to the corrosion rate at the same velocity of the multiphase fluids passing through typical REAC systems or even sour water (single phase, liquid full) flowing through typical pipe sizes in these systems. Wall shear stress was chosen as the scaling parameter in order to make the appropriate comparison.

The wall shear stress for the system in service can be calculated for the specific tube or pipe size, throughput, flow regime and fluid physical properties and correlated with a corresponding laboratory flow loop velocity that produces the same value of wall shear stress. For a 100% liquid sour water system, the wall shear stress produced in 2-inch NPS (60-mm nominal OD) to 6-inch NPS (168-mm nominal OD) piping can be achieved at much lower velocities in the small diameter flow-through coupons utilized in the laboratory flow loop. For example, the shear stress related to 17 ft/s (5.2 m/s) flow in a 4-inch NPS (114-mm nominal OD) pipe can be achieved at 10 ft/s (3.0 m/s) in the 0.15-inch ID (3.8-mm) bore flow-through coupon used in the laboratory study. Any given velocity of sour water in the small bore flow-through coupons in the laboratory test produces a much higher wall shear stress than in common sizes of sour water piping in the field. While the example relationship discussed above applies to a 100% liquid sour water flow, even greater differences may be present in multiphase flow conditions. The corrosion prediction software tool developed as part of this JIP readily makes this wall shear stress – velocity correlation.

These isocorrosion curves have already had a profound impact on the refinery industry as a result of the JIP sponsor usage. They represent the first comprehensive set of NH_4HS corrosion data available to the industry for use in evaluating corrosion in, and selecting materials of construction for, various process units containing alkaline sour water.

Effect of H_2S Partial Pressure

The data collected in this subtask were intended to investigate the role that H_2S partial pressure plays in NH_4HS corrosion. The test matrix for this subtask included 28 tests that were conducted at P_{H2S} = 30 psia (210 kPa absolute), 100 psia (690 kPa absolute) and 150 psia (1,000 kPa absolute) for comparison with the baseline data at P_{H2S} = 50 psia (340 kPa absolute).

The results of this subtask proved that H_2S partial pressure has a significant effect on the corrosion rate in H_2S-dominated sour water systems. When the data were plotted as corrosion rate versus H_2S partial pressure for each of the NH_4HS concentrations tested, the plots yielded a fan-shaped appearance. Corrosion rate increased with a corresponding increase in H_2S partial pressure at each NH_4HS concentration. The corrosion rate increase was more pronounced at higher NH_4HS concentrations. This relationship is clearly illustrated in Figure 3 for carbon steel in the tests conducted at 20 ft/s (6.1 m/s). The effect of H_2S partial pressure was measured at other test velocities including static conditions. It is critical to note that the magnitude of the effect differed for each condition. The differing behavior produced rule sets incorporating curves at the different test velocities to correct the baseline corrosion rate (from the isocorrosion diagram) of each material for the effect of H_2S partial pressure that are used in the corrosion prediction software tool.

Several observations were made regarding the influence of H_2S partial pressure. H_2S partial pressure had a significant effect on the corrosion of carbon steel and all the alloys tested. The corrosion rates of carbon steel, type 410 (UNS S41000) stainless steel, type 304 stainless steel, type 316 stainless steel and alloy 2205 at 100 psia (690 kPa absolute) and 150 psia (1,000 kPa absolute) H_2S were all significantly higher than their respective corrosion rates at 50 psia (340 kPa absolute) H_2S. Alloy 2205, alloy 800 (UNS N08800) and alloy 600 (UNS N06600) demonstrated comparable corrosion resistance that was only marginally better than type 304 stainless steel at high H_2S partial pressure.

Alloy 825, alloy 20Cb-3 (UNS N08020) and alloy 625 (UNS N06625) were somewhat more corrosion resistant than alloy 2205, alloy 800 and alloy 600 at high H_2S partial pressure. The measured corrosion rates for alloy 825, alloy 20Cb-3 and alloy 625 showed a dramatic increase over the very low corrosion rates measured at 50 psia (340 kPa absolute) H_2S. This raised concern about the useful resistance of these alloys at high H_2S partial pressure, especially at the higher NH_4HS concentrations.

Alloy 2507 (UNS S32750) and UNS N08367 were far more corrosion resistant than alloy 2205 and the previously mentioned nickel-based alloys at high H_2S partial pressure. Alloy C-276 was the best of class, with measured corrosion rates < 2 mpy (0.05 mm/y) up to 20 wt% NH_4HS at 150 psia (1,000 kPa absolute) H_2S partial pressure.

Using the data obtained in the first task of the JIP, a general ranking of material resistance to NH_4HS corrosion in H_2S-dominated alkaline sour waters was developed. The materials were ranked individually from least resistant to most resistant. This relative ranking was affectionately referred to as the “pony plot” in the JIP sponsor meetings. This “pony plot” is presented in Figure 4.

H_2S partial pressure proved to be a major variable that must be considered when assessing the potential for NH_4HS corrosion of all materials tested in alkaline sour water environments. Prior to this JIP, the focus on assessing NH_4HS corrosion had been on only two variables - NH_4HS concentration and velocity. The key learnings from this first task indicate the inadequacies of that focus. The results

of this task confirm the following conclusions regarding assessment of NH_4HS corrosion for all materials in H_2S-dominated sour water systems:

a) NH_4HS concentration is a key variable.

b) Velocity is a key variable within a given section of a system, but it is important to realize that it is not the correct parameter that permits direct correlation between different systems or even different portions of the same system, especially between liquid-full sour water systems and multiphase systems. Wall shear stress is a much better scaling parameter for this purpose.

c) H_2S partial pressure is another key variable that must be considered.

Effect of Temperature

The test matrix for this subtask included 16 tests to investigate the role of temperature on the corrosion rate in H_2S-dominated NH_4HS environments. The test matrix involved NH_4HS concentrations that varied from 1 to 8 wt%, test velocities of 20 ft/s (6.1 m/s) and 80 ft/s (24 m/s), H_2S partial pressures of 50 psia (340 kPa absolute) and 100 psia (690 kPa absolute), and temperatures of 190°F (88°C) and 250°F (121°C) for comparison with the results of the previous tests conducted at 130°F (55°C).

The results of this subtask confirmed that increased temperature produced an increase in corrosion rate of carbon steel and all alloys tested, as expected. The effect of temperature on the corrosion rate of carbon steel, alloy 400, type 410 stainless steel and alloy 2205 was greatest at low NH_4HS concentration (~ 2 wt%), and diminished as the NH_4HS concentration increased. For the other alloys tested, the peak effect of temperature shifted progressively to higher NH_4HS concentrations as the alloy corrosion resistance increased.

These data quantified the effect of temperature on the NH_4HS corrosion rate of all materials and were used to develop rule sets to correct the baseline corrosion rate (from the isocorrosion diagram) of each material for the effect of temperature that are used in the corrosion prediction software tool.

Although the effect of temperature is certainly an important and necessary consideration when assessing the potential for NH_4HS corrosion, it was judged to be of secondary importance to the effect of the three key variables mentioned previously – NH_4HS concentration, velocity (wall shear stress), and H_2S partial pressure.

Effect of Chloride Concentration

The test matrix for this subtask included 16 tests to investigate the role of chloride on the corrosion rate in H_2S-dominated NH_4HS environments. The test matrix involved NH_4HS concentrations that varied from 1 to 15 wt%, test velocities of 20 ft/s (6.1 m/s) and 80 ft/s (24 m/s), H_2S partial pressures of 50 psia (340 kPa absolute), temperature of 130°F (55°C) and chloride concentrations of 100 and 1,000 ppm for comparison with the results of the previous tests conducted with 0 ppm chloride.

The addition of HCl to attain the desired chloride concentration was anticipated to result in a decrease in pH that might result in increased corrosiveness. However, these NH_4HS solutions are highly buffered and the pH change caused by the addition of HCl to achieve the 1,000 ppm chloride level was determined by ionic modeling to be negligible (< 0.01 pH unit).

The data obtained at 100 ppm chloride were compared to those obtained at 1,000 ppm chloride for carbon steel and the alloys investigated in this subtask. No differences in corrosion rate were observed that could be attributed to the presence of chloride in the sour water. Comparison of these data at 100 and 1,000 ppm chloride with data collected in previous tasks containing 0 ppm chloride agreed in most cases up to 10 wt% NH_4HS. However, at 15 wt% NH_4HS, the 0 ppm chloride sour water exhibited higher corrosion rates than sour waters containing 100 and 1,000 ppm chlorides, particularly at the test velocity of 80 ft/s (24 m/s). A number of tests were repeated to confirm the corrosion rates determined in the presence of chlorides. These tests yielded similar results.

Based on the results obtained in this subtask, it was concluded that the presence of chloride at concentrations up to 1,000 ppm in the sour water did not increase the corrosion rate of carbon steel or the alloys tested. Therefore, the baseline corrosion rate (from the isocorrosion diagram) of each material was not adjusted for the effect of chloride concentration in the corrosion prediction software tool.

Effect of Hydrocarbon / Sour Water Mixtures

The test matrix for the third task was developed to investigate the role of hydrocarbon on the corrosion rate in NH_4HS environments. It is known that the presence of hydrocarbon can have an inhibiting effect, thereby reducing the corrosion rate. The decrease in corrosion rate results from reducing the time the corrosive sour water phase contacts the metal surface, as the wettability of the hydrocarbon restricts the ability of the sour water to contact and corrode the metal surface.

The presence of hydrocarbon can increase the corrosion rate above that for 100 vol% sour water as a result of increasing the shear stress produced at the metal surface under flowing conditions. This behavior obviously becomes a greater possibility as the density and viscosity of the hydrocarbon increase. It also shows the added importance of assessing the corrosiveness of the flowing multiphase fluid based on the wall shear stress and not the linear flow velocity.

To investigate these phenomena, the test matrix for this task incorporated both light and heavy hydrocarbons. Experiments covered hydrocarbon contents in the range of 10 to 98 vol%, with 0 vol% data available from the first task for comparison. All testing was conducted at 130°F (55°C) and two H_2S partial pressures, 50 psia (340 kPa absolute) and 100 psia (690 kPa absolute). The effect of wall shear stress on the corrosion performance was also examined with the heavy hydrocarbon.

The heavy hydrocarbon chosen for study in this task was a naphthenic process oil with an API gravity of 20. The light hydrocarbon chosen for study was a dearomatized aliphatic performance fluid with an API gravity of 40. Selected properties for the two hydrocarbons are provided in Table 3. In addition to these properties, density and viscosity were measured over the temperature range of 100 – 250°F (38 – 121°C). These data were collected to provide accurate properties for use in the flow modeling conducted as part of the experiments and to provide a set of properties for use in the corrosion prediction software tool.

The corrosion data collected for carbon steel using various volume fractions of the heavy hydrocarbon indicated that substantial protection from the presence of heavy hydrocarbon was not achieved until the hydrocarbon content exceeded 25 vol%. A strong dependence on the H_2S partial pressure was also observed in the data collected at 0 and 10 vol% heavy hydrocarbon. This further

supported the prior conclusion that increased H_2S partial pressure results in a dramatic increase in the corrosion rate. The corrosion data collected for carbon steel using various volume fractions of the light hydrocarbon indicated similar results to the heavy hydrocarbon.

A similar analysis was performed on the five alloy materials included in this task. The main difference observed between the performance of the alloys and carbon steel was that substantial protection from the presence of hydrocarbon was experienced with the alloys at lower hydrocarbon contents than that observed for carbon steel.

To model the influence of the hydrocarbon, the efficiency of protection was determined for each data point. The efficiency of protection was calculated by subtracting the ratio of the corrosion rate obtained with the presence of hydrocarbon to the corrosion rate obtained in the corresponding 100 vol% sour water test environment with 0 vol% hydrocarbon (expressed as a percentage) from 100%. This is a similar treatment used to evaluate inhibitor effectiveness. Efficiency of protection for carbon steel increased rapidly up to approximately 25 vol% hydrocarbon. Beyond that the efficiency increased gradually until it approached almost complete protection at very high vol% hydrocarbon. The efficiency of protection calculated for the five alloy materials tested showed similar behavior except that the inflection point occurred at lower vol% hydrocarbon and efficiency of protection value at the inflection point varied for the different alloy materials.

The relationship between efficiency of protection versus hydrocarbon content was used to correct the 100 vol% sour water corrosion rates for the presence of hydrocarbon in multiphase systems in the corrosion prediction software tool. The flow regime was an important consideration that must be included in corrosion prediction. The efficiency of protection benefit for the presence of hydrocarbon was only taken for turbulent flow regimes that would cause the tube/pipe wall inner surfaces to be continuously wetted by hydrocarbon. For laminar, stratified or wave flow regimes, some portion of the tube/pipe internal surface would be wetted by the sour water phase alone, and not by the hydrocarbon phase. In these cases, no benefit for the presence of the hydrocarbon was taken.

Effect of Wall Shear Stress. Due to the higher density and viscosity of the heavy hydrocarbon, the effect of wall shear stress could also be studied. The wall shear stress in the laboratory flow-through test coupons associated with 100 vol% sour water at 50 ft/s (15 m/s) was 510 Pa. With test mixtures of the heavy hydrocarbon and sour water, wall shear stress equivalent to four times this value could be attained (i.e., 2,040 Pa). The results indicated that the higher shear stress produced a higher corrosion rate at a given set of environmental test conditions. The magnitude of the corrosion rate difference was also a function of the corrosiveness of the test environment. At lower hydrocarbon contents, the test environment was primarily sour water and the increased wall shear stress had a greater influence on increasing the corrosion rate. At higher hydrocarbon contents, less sour water was present and the corrosion rate difference between the two wall shear stresses was small.

Performance of Chemical Treatments

The test matrix for the fourth task was developed to investigate the role of two chemical treatments, ammonium polysulfide (APS) and imidazoline, on reducing the corrosion rate in NH_4HS environments. The efficiency of protection was calculated for all corrosion rate data collected in this task, similar to the approach used for analysis of the hydrocarbon/sour water mixture results discussed above.

Ammonium Polysulfide. Efficiency of protection of 75 – 90% was attained with various concentrations of APS at a test velocity of 20 ft/s (6.1 m/s). However, an important point in corrosion prediction is that the efficiency of protection attained with APS varied with test velocity. At all treatment levels of APS tested, the efficiency of protection was greater at 20 ft/s (6.1 m/s) than at 80 ft/s (24 m/s). These results indicate that the APS can form a more stable protective film on the metal surface at lower velocities (wall shear stresses). At higher velocities (wall shear stresses), this protective film becomes less stable resulting in reduced protection. The relationship between efficiency of protection versus the APS treatment level and velocity was used to correct the untreated sour water corrosion rates in the corrosion prediction software tool.

Imidazoline. The data collected using imidazoline showed a higher degree of variability than the data collected with APS. Efficiency of protection attained with imidazoline varied from approximately 35 – 95%. Also, the test results with imidazoline did not follow the same trend with test velocity that was observed with APS. Although many of the tests conducted with imidazoline at 80 ft/s (24 m/s) resulted in higher efficiencies of protection than those tests run at 20 ft/s (6.1 m/s), trends were not as clear as the those observed with APS. Because imidazoline is a hydrocarbon-soluble chemical, its ability to protect carbon steel exposed to the corrosive sour water environment was considered questionable for certain multiphase flow regimes.

The observed behavior in the imidazoline tests was explained on the basis of mixing. Imidazoline is soluble in hydrocarbon but not in water. Because these tests were conducted in the absence of hydrocarbon, the imidazoline was diluted with 0.5 vol% isopropyl alcohol to increase the solubility in the sour water. However, this did not make the imidazoline water-soluble. As a result, tests conducted at 80 ft/s (24 m/s) provided better mixing of the test liquids and assisted in increasing the contact of the imidazoline with the metal surfaces. At lower test velocities, separation of the imidazoline phase probably occurred and resulted in decreased efficiency of protection. For this reason, the upper and lower bounds to the efficiency of protection data (regardless of velocity) were used to represent most and least conservative relationships. These relationships for the efficiency of protection versus the imidazoline concentration were used to correct the untreated sour water corrosion rates in the corrosion prediction software tool. Application of the most and least conservative relationships was based on the multiphase flow regime, considering the ability of the imidazoline to wet the entire internal surface of the tube/pipe. For some flow regimes (e.g., stratified, laminar), no credit was given (i.e., efficiency of protection = 0) for the presence of imidazoline regardless of its concentration.

Carbon steel was the only material evaluated in this task. The ability of APS and imidazoline to provide corrosion protection on the 13 alloy materials is unknown. Hence, only the corrosion rate of carbon steel was corrected in the corrosion prediction software tool for the presence of APS or imidazoline.

NH_4HS Corrosion Prediction Software Tool

The fifth task of this JIP was to develop a user-friendly software tool to predict NH_4HS corrosion rates. The corrosion prediction software tool developed for this purpose is called Predict®-SW.[5] This user-friendly software tool successfully incorporated the data obtained in the JIP and combined these data with flow modeling calculations on plant tube/pipe configurations to predict the corrosion rates of the 14 materials studied over a wide range of NH_4HS concentration, H_2S partial pressure, temperature, hydrocarbon content and chemical treatment.

[5] Software product of InterCorr International, Inc. (now Honeywell Process Solutions)

This software tool is described in more detail, along with reviews of several case studies where its application has provided significant economic benefit, in a separate paper by Cayard et al.[8]

CONCLUSIONS

The following conclusions relating to H_2S-dominated alkaline sour water systems were drawn from the results of this program.

1. Three discrete NH_4HS corrosion regimes were indicated by the location and shape of the isocorrosion curves on the isocorrosion diagram developed for carbon steel:

   a. At low NH_4HS concentrations (2 wt% or less), low corrosion rates were observed at low velocity. Corrosion rates increased only marginally with increased velocity.

   b. At intermediate NH_4HS concentrations (2 – 8 wt%), low to moderate corrosion rates were observed at low velocity. Corrosion rates increased markedly with increased velocity.

   c. At high NH_4HS concentrations (greater than 8 wt%), moderate to high corrosion rates were observed at low velocity. Corrosion rates increased markedly with increased velocity.

2. The isocorrosion curves on the isocorrosion diagrams developed for the alloy materials tested were shifted upwards and toward the right, indicating the increase in material resistance as compared with carbon steel.

3. H_2S partial pressure has a significant effect on the corrosion of carbon steel and all the alloys tested. The corrosion rates of carbon steel and several of the alloys at P_{H2S} = 100 – 150 psia (690 – 1,000 kPa absolute) were significantly higher than their respective corrosion rates at P_{H2S} = 50 psia (340 kPa absolute).

4. H_2S partial pressure proved to be a major variable that must be considered when assessing the potential for NH_4HS corrosion in alkaline sour water environments. Prior to this JIP, the focus on assessing NH_4HS corrosion had been on only two variables - NH_4HS concentration and velocity. Key learnings from this JIP indicate the inadequacies of that focus. Assessment of the potential for NH_4HS corrosion in H_2S-dominated sour water systems must include H_2S partial pressure as the third key variable.

5. Test results do not support the continued use of the 20 ft/s (6.1 m/s) velocity limit for controlling NH_4HS corrosion of carbon steel. That limit is too conservative at low NH_4HS concentrations and low H_2S partial pressures, and too liberal at high NH_4HS concentrations and high H_2S partial pressures. Furthermore, it does not adequately account for differences resulting from multiphase flow regimes present in most REAC systems. Wall shear stress was found to be a much better scaling parameter than velocity for correlating corrosion performance of materials.

6. Despite the current widespread belief that two commonly used materials – alloy 2205 and alloy 825 – are suitable to mitigate corrosion in REAC systems, both of these materials were found to corrode at intermediate and high NH_4HS concentrations, especially at high velocities and high H_2S partial pressures.

7. A general ranking of resistance to NH_4HS corrosion in H_2S-dominated sour waters was developed for all materials tested. Alloy 2507 and UNS N08367 were found to be far more corrosion resistant than alloy 2205 and many of the nickel-based alloys, especially at high H_2S partial pressure. Alloy C-276 was found to be the most corrosion resistant material evaluated in this program.

8. The corrosion rates of carbon steel and all alloys evaluated in this program increased with increasing temperature. The effect of temperature on the corrosion rate of carbon steel was greatest at low NH_4HS concentrations, and diminished as the NH_4HS concentration increased. Temperature appeared to have less effect on corrosion than NH_4HS concentration, velocity (wall shear stress), and H_2S partial pressure.

9. Presence of chloride at concentrations up to 1,000 ppm in the sour water did not increase the corrosion rate of carbon steel or the alloys tested.

10. The presence of hydrocarbon mixed with sour water resulted in reduced corrosion rates when compared to 100 vol% sour water. Substantial protection was achieved for carbon steel at hydrocarbon contents ≥ 25 vol%. Substantial protection was achieved for the alloys tested at lower hydrocarbon contents.

11. Addition of 50 – 500 ppmv ammonium polysulfide (APS) successfully reduced the NH_4HS corrosion rate of carbon steel by 75 – 90%. At low velocity (wall shear stress), APS formed a more stable protective film on the metal surface that led to greater protection. At higher (wall shear stress), this film became less stable resulting in reduced protection.

12. Addition of 100 – 500 ppmv imidazoline reduced the NH_4HS corrosion rate of carbon steel by 35 – 95%, but showed a high degree of variability. The successful results with imidazoline relied on sufficient mixing to ensure contact of the imidazoline with the metal surface. Thus, the potential reduction of corrosion when using imidazoline may not be realized with certain flow regimes, particularly stratified or laminar flow.

13. A user friendly software tool was developed that successfully incorporated the data obtained in this program and combined these data with flow modeling calculations on plant tube/pipe configurations to predict the corrosion rates of the 14 materials studied over a wide range of NH_4HS concentration, H_2S partial pressure, temperature, hydrocarbon content and chemical treatment.

ACKNOWLEDGMENTS

The authors would like to acknowledge the support and contributions to this program by many of our industry colleagues, especially all the representatives of the Sour Water JIP sponsor companies. We would also like to specifically acknowledge Ashok Dewan, Mary Ann Moore, and Paul Petkovsky of Shell Global Solutions (US) Inc. for their ionic modeling work, and Larry Zimmerman of Shell Global Solutions (US) Inc. and Ken Schindler and Lou Hajdik of InterCorr International, Inc. for their skill and dedicated efforts in safely conducting these very challenging laboratory tests.

TABLE 1
MATERIALS EVALUATED AND NOMINAL COMPOSITIONS

Material	UNS Number	%C	%Cr	%Mn	%Mo	%Ni	%Cu	%Fe	%Cb	%Co
Carbon Steel	G10180	0.15-0.20	-	0.6-0.9	-	-	-	bal	-	-
Alloy 400	N04400	0.3 max	-	2.0 max	-	63-70	bal	2.5 max	-	-
Type 410 SS	S41000	0.015 max	11.5-13.5	1.0 max	-	-	-	bal	-	-
Type 304 SS	S30400	0.08 max	18-20	2.0 max	-	8-10.5	-	bal	-	-
Type 316 SS	S31600	0.08 max	16-18	2.0 max	2-3	10-14	-	bal	-	-
Alloy 2205	S31803	0.03 max	21-23	2.0 max	2.5-3.5	4.5-6.5	-	bal	-	-
Alloy 800	N08800	0.1 max	19-23	1.5 max	-	30-35	0.75 max	bal	-	-
Alloy 600	N06600	0.15 max	14-17	1.0 max	-	72 min	0.5 max	6-10	-	-
Alloy 20Cb-3	N08020	0.07 max	19-21	2.0 max	2-3	32-38	3-4	bal	-	-
Alloy 825	N08825	0.05 max	19.5-23.5	1.0 max	2.5-3.5	38-46	1.5-3.0	bal	-	-
Alloy 625	N06625	0.1 max	20-23	0.5 max	8-10	bal	-	5.0 max	3.15-4.15	-
Alloy 2507	S32750	0.03 max	24-26	1.2 max	3-5	6-8	-	bal	-	-
6% Mo super-austenitic SS	N08367	0.03 max	20-22	2.0 max	6-7	23.5-25.5	-	bal	-	-
Alloy C-276	N10276	0.02 max	14.5-16.5	1.0 max	15-17	bal	-	4-7	-	2.5 max

TABLE 2
PREDICTED VS. MEASURED pH

NH_4HS Conc. (%w)	Predicted pH 77°F (25°C)	Measured pH Room Temperature
1	6.90	6.87, 6.92, 6.92, 6.92
2	7.18	7.13, 7.17, 7.22, 7.16
5	7.57	7.66, 7.59, 7.66, 7.63
8	7.83	7.85, 7.89, 7.87, 7.87
10	7.98	8.01, 8.05, 8.05, 8.08
15	8.32	8.36, 8.36, 8.38, 8.41
20	8.60	8.64, 8.64, 8.67, 8.63
30	9.11	9.13, 9.20, 9.03, 9.21

Note: 50 psia (340 kPa absolute) H_2S partial pressure

TABLE 3
PROPERTIES OF LIGHT AND HEAVY HYDROCARBONS

Property	Light Hydrocarbon	Heavy Hydrocarbon
Distillation Range	407 – 455°F (208 – 235°C)	557 – 1001°F (292 – 538°C)
Flash Point	181°F (83°C)	430°F (221°C)
Specific Gravity @ 60°F (15°C)	0.798	0.934
API Gravity	40	20

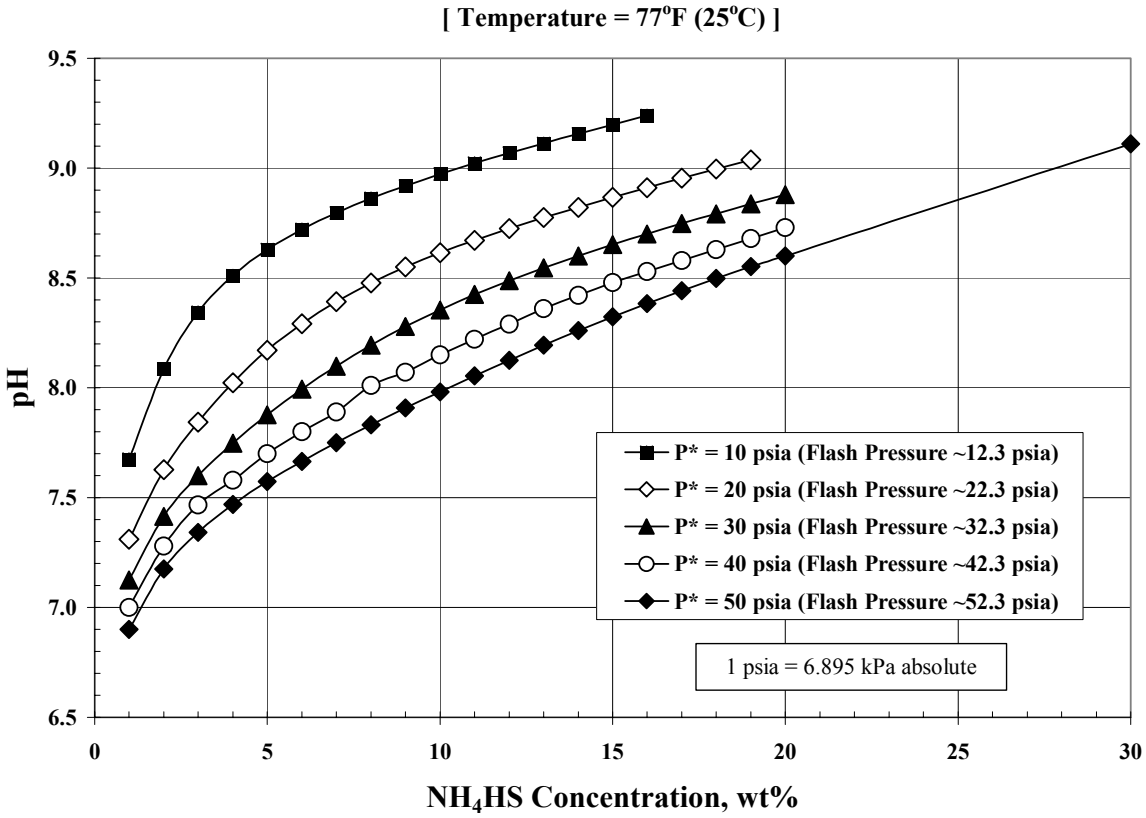

FIGURE 1 – Predicted pH vs. NH_4HS Concentration Using the Ionic Model

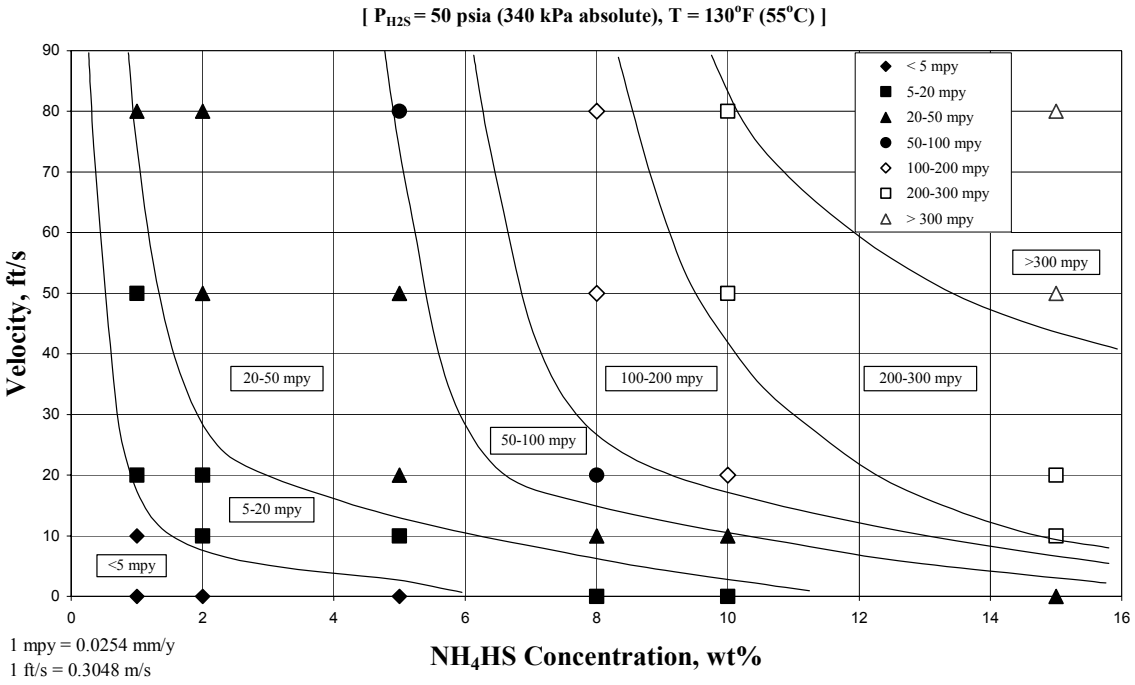

FIGURE 2 – Isocorrosion Diagram for Carbon Steel

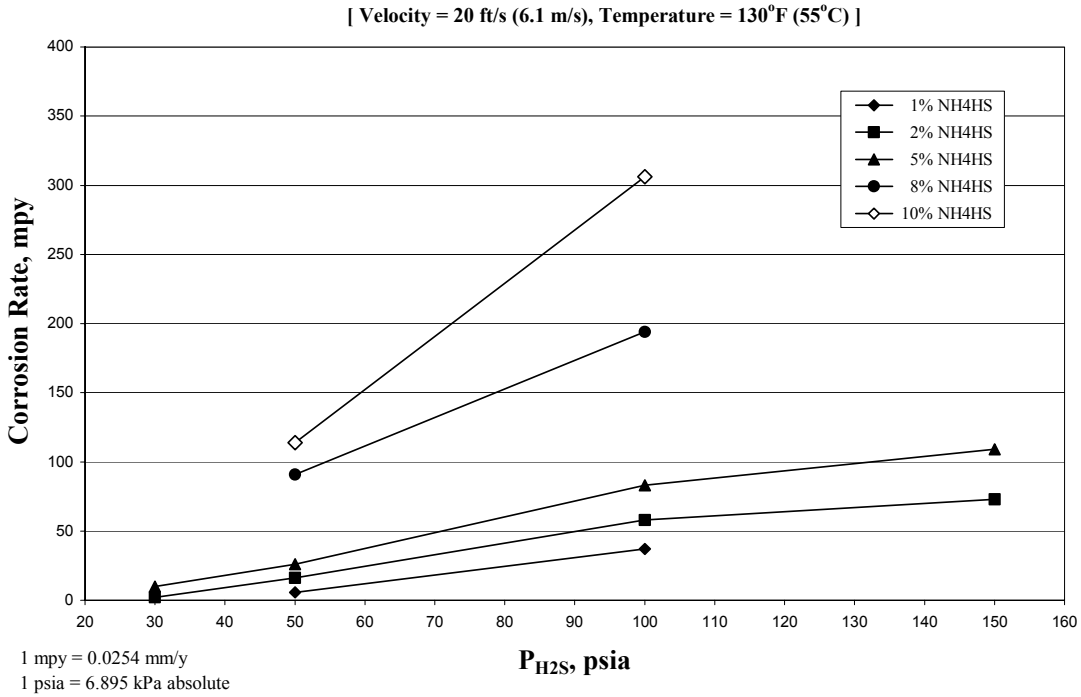

FIGURE 3 – Effect of H_2S Partial Pressure on NH_4HS Corrosion of Carbon Steel

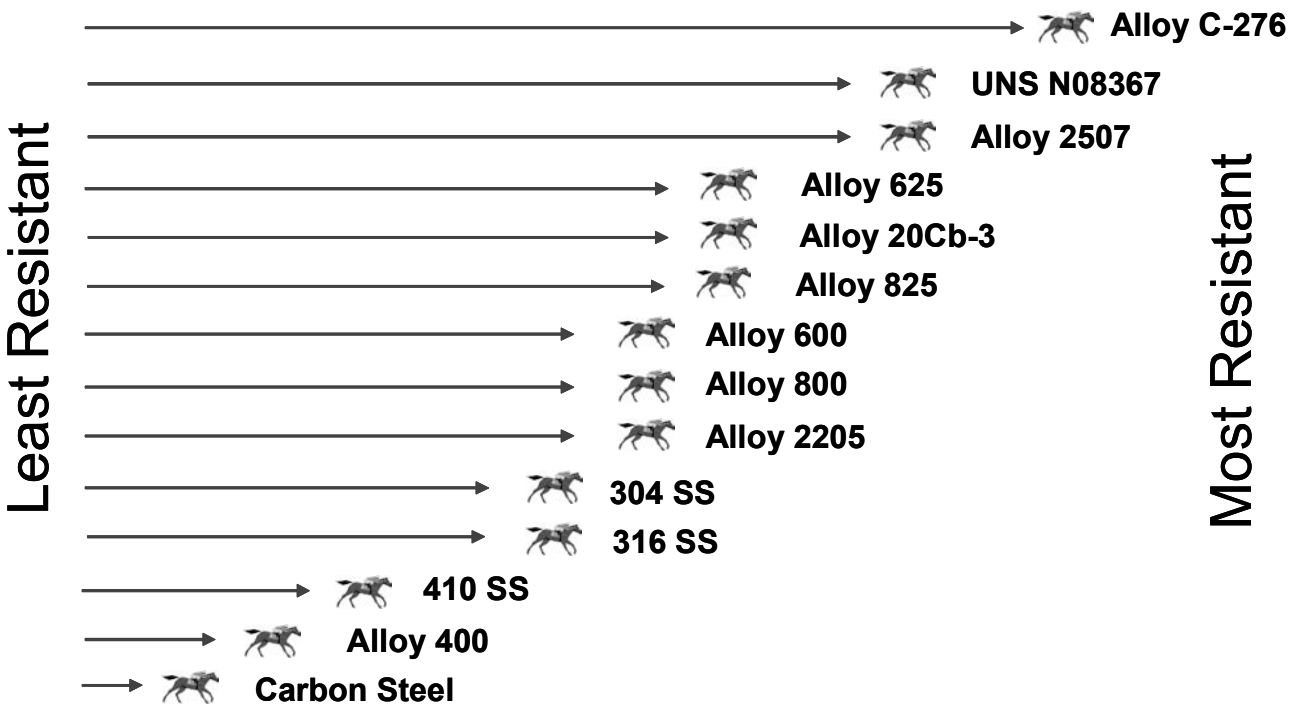

FIGURE 4 – Material Resistance to NH_4HS Corrosion

REFERENCES

1. ASM Handbook, Volume 13, Corrosion, ASM International, 1987.

2. R.L. Piehl, "Survey of Corrosion in Hydrocracker Effluent Air Coolers", Materials Performance, Vol 15 (1), January 1976, pp 15-20.

3. D.G. Damin and J. D. McCoy, "Prevention of Corrosion in Hydrodesulfurizer Air Coolers and Condensers", Materials Performance, Vol 17 (12), December 1978, pp 23-26 (see also NACE CORROSION/78, paper no. 131).

4. C. Scherrer, M. Durrieu, and G. Jarno, "Distillate and Resid Hydroprocessing: Coping with High Concentrations of Ammonium Bisulfide in the Process Water", Materials Performance, Vol 19 (11), November 1980, pp 25-31 (see also NACE CORROSION/79, paper no. 27).

5. API Publication 932-A, "A Study of Corrosion in Hydroprocess Reactor Effluent Air Cooler Systems", (Washington, DC: American Petroleum Institute, September 2002).

6. R.D. Kane and M.S. Cayard, "Prediction and Assessment of Ammonium Bisulfide Corrosion Under Refinery Sour Water Service Conditions – Phase 1," InterCorr International, Inc., Joint Industry Program Proposal, Revision 3, March 20, 2001.

7. Private Communication: Michael S. Cayard, InterCorr International, Inc., and Richard J. Horvath, Shell Global Solutions (US) Inc., "Final Report on Prediction and Assessment of Ammonium Bisulfide Corrosion Under Refinery Sour Water Service Conditions – Phase 1", Issued by InterCorr International, Inc. to the Sour Water JIP Sponsors, June 10, 2003.

8. M.S. Cayard, W.G. Giesbrecht, R.J. Horvath, R.D. Kane and V.V. Lagad, "Prediction of Ammonium Bisulfide Corrosion and Validation with Refinery Plant Experience," CORROSION/2006, paper no. 06577 (Houston, TX: NACE, 2006).